

# Kick velocity induced by magnetic dipole and quadrupole radiation

Yasufumi Kojima\* and Yugo E. Kato

*Department of Physics, Hiroshima University, Higashi-Hiroshima 739-8526, Japan*

\* `kojima@theo.phys.sci.hiroshima-u.ac.jp`

## ABSTRACT

We examine the recoil velocity induced by the superposition of the magnetic dipole and quadrupole radiation from a pulsar/magnetar born with rapid rotation. The resultant velocity depends on not the magnitude, but rather the ratio of the two moments and their geometrical configuration. The model does not necessarily lead to high spatial velocity for a magnetar with a strong magnetic field, which is consistent with the recent observational upper bound. The maximum velocity predicted with this model is slightly smaller than that of observed fast-moving pulsars.

*Subject headings:* stars: magnetic field — stars: neutron — pulsars: general

## 1. INTRODUCTION

The surface magnetic field strength  $B_s$  of a pulsar is conventionally estimated by matching the rotational energy loss rate with the magnetic dipole radiation rate, that is,  $B_s \approx (3c^3 IP \dot{P})^{1/2} / (2\sqrt{2}\pi R_s^3)$ , where  $I$  is the inertial moment,  $R_s$  is the stellar radius,  $P$  is the spin period, and  $\dot{P}$  is the time derivative of the spin period. The precision of this approximation is only at the order of magnitude level because actual energy loss is not well described by magnetic dipole radiation in a vacuum. A more realistic model with current flows and radiation losses is required, but has not yet been established. A simple estimate provides  $B_s \approx 10^{12}$  G for typical radio and X-ray pulsars, and  $B_s \approx 10^{13}$ - $10^{15}$  G for magnetars, although the level of the approximation must be noted. Dynamo action in a rapidly rotating proto-neutron star with  $P \approx 1$  ms is proposed as a mechanism for this amplification by 2-3 orders of magnitude (see e.g., Thompson & Duncan (1993); Bonanno, Rezzolla & Urpin (2003); Bonanno, Urpin & Belvedere (2006)). Actual upper limit of  $B_s$  generated in the convective proto-neutron star is estimated as  $10^{15} - 10^{16}$  G, beyond which all sorts of instabilities are suppressed by strong magnetic fields (Miralles, Pons & Urpin 2002).

Recent numerical simulations of dynamo action can be used to study the large-scale fields in fully convective rotating stars. For example, non-axisymmetric fields are generated in the case of uniform rotation (Chabrier & Küker 2006), while mostly axisymmetric fields with a mixture of the first few multipoles are formed in the case of a differentially rotating star (Dobler, Stix & Brandenburg 2006). The results may not directly apply to pulsars or magnetars, but suggest that the magnetic

field configuration of neutron stars may not be an ordered dipole. If there are higher-order multipoles, these will also contribute to the radiation loss. The upper bounds on their surface magnetic fields are rather loose. See Krolik (1991) for a discussion of the magnetic fields of millisecond pulsars. The magnetic field strength  $B_{lm}$  relevant to the multipole moment of order  $(l, m)$  is limited to  $B_{lm} \leq B_s / (m R_s \Omega / c)^{l-1}$ , where  $\Omega = 2\pi/P$  is angular velocity, and the radiation of each multipole  $L_{lm} \sim c(m R_s \Omega / c)^{2l+2} (B_{lm} R_s)^2$  is assumed to be smaller than that of a dipole. Thus, a model with complex magnetic configuration at surface  $B_{lm} \geq B_s$  ( $l > 1$ ) is allowed because of the small factor  $R_s \Omega / c \ll 1$  for observed stars.

Some proto-neutron stars are conjectured to be born in hypothetical extreme state of rapid rotation  $P \approx 1$  ms with an ultra strong magnetic field  $B_s \approx 10^{15}$  G. Is there any remaining evidence of this stage? The proper motion can possibly be used as a probe. Several kick mechanisms operative at the core bounce of a supernova explosion have been proposed to date: anisotropic emissions of neutrinos (e.g., Arras & Lai (1999); Fryer & Kusenko (2006)), hydrodynamical waves (e.g., Scheck et al. (2006)), and MHD effects (e.g., Sawai, Kotake & Yamada (2008)). These mechanisms operate on a dynamical timescale of the order of milliseconds or the cooling timescale of  $\sim 10$  s. If the strong magnetic fields are generated on a longer timescale, some natal kick mechanisms involved the magnetic-field-driven anisotropy do not work effectively. Recoil driven by electromagnetic radiation, which is operative on a longer spindown timescale of  $\sim 10^3 (B/10^{15} \text{ G})^{-2} (P_i/1 \text{ ms})^2$  s, has been proposed as a post-natal kick mechanism (Harrison & Tademaru 1975) (see also Lai, Chernoff & Cordes (2001) for the corrected expression). In their model, an oblique dipole moment displaced by a distance  $s$  from the stellar center rotates. This causes the radiation of higher order multipoles, whose superposition is generally asymmetric in the spin direction, leading to the kick velocity. In the off-center model, the quadrupole field  $B_2$  of order  $B_2 \sim (s/R_s) \times B_1 \sim B_1$  is involved. It is interesting to study the case where  $B_2 \gg B_1$ , because the constraint of the higher order component by the radiation is very weak, for example,  $B_2 \sim (c/(R_s \Omega)) \times B_1 \gg B_1$ . In this paper, we revisit the kick velocity induced by electromagnetic radiation from a magnetized rotating star with both dipole and quadrupole fields, in which a larger quadrupole field  $B_2 \gg B_1$  at the surface is allowed.

This paper is organized as follows. In Section 2, we present the radiation from rotating dipole and quadrupole moments in vacuum. Their field strength and inclination angle with respect to the spin axis are arbitrary. We also compare our model with the off-centered dipole model. In Section 3, we evaluate the maximum kick velocity as a recoil of momentum radiation. Section 4 presents our conclusions.

## 2. MODEL

### 2.1. Electromagnetic Fields

We consider electromagnetic fields outside a rotating object with angular frequency  $\Omega$ ; the object has a magnetic dipole and quadrupole moments. The dipole moment is denoted by  $\mu$ , and

the direction is inclined from the spin axis by  $\chi_1$ . Quadrupole moment is denoted by  $Q$  and the inclination angle of the symmetric axis is  $\chi_2$  from the spin axis. The electromagnetic fields outside the rotating magnetized object are described by the magnetic multipoles of order  $l = 1, 2, |m| \leq l$ , for which  $E_r = \mathbf{E} \cdot \mathbf{r} = 0$  (Jackson 1975). The explicit components produced by the rotating dipole moment are given by

$$B_r = \frac{2\mu}{r^3} \left[ P_1^0(\chi_1)P_1^0(\theta) + P_1^1(\chi_1)P_1^1(\theta)S_1(\xi)e^{i\lambda} \right], \quad (1)$$

$$B_\theta = -\frac{\mu}{r^3} \left[ P_1^0(\chi_1)P_1^{\prime 0}(\theta) + P_1^1(\chi_1)P_1^{\prime 1}(\theta)S_2(\xi)e^{i\lambda} \right], \quad (2)$$

$$B_\phi = -\frac{i\mu}{r^3} P_1^1(\chi_1)S_2(\xi)e^{i\lambda}, \quad (3)$$

$$E_\theta = -\frac{\mu\Omega}{cr^2} P_1^1(\chi_1)S_1(\xi)e^{i\lambda}, \quad (4)$$

$$E_\phi = -\frac{i\mu\Omega}{cr^2} P_1^1(\chi_1)P_1^{\prime 1}(\theta)S_1(\xi)e^{i\lambda}, \quad (5)$$

where  $\lambda = \phi - \Omega(t - r/c)$ . The function  $P_l^m(x)$  is the associated Legendre function and the prime denotes the derivative with respect to  $x$ . The function  $S_n$ , which is derived from the spherical Hankel function, is a polynomial of  $\xi = \Omega r/c$ , and is explicitly written as

$$S_1(\xi) = 1 - i\xi, \quad (6)$$

$$S_2(\xi) = 1 - i\xi - \xi^2. \quad (7)$$

We here use convenient complex expressions in eqs. (1)-(5) and the actual fields are the real part. Near the stellar surface  $R_s \leq r \ll c/\Omega$ , magnetic field for eqs.(1)-(3) at the phase  $e^{i\lambda} = 1$  reduces to

$$\mathbf{B} = \frac{2\mu}{r^3} \cos(\theta - \chi_1) \mathbf{e}_r + \frac{\mu}{r^3} \sin(\theta - \chi_1) \mathbf{e}_\theta = -\nabla \left( \frac{\mu}{r^2} \cos(\theta - \chi_1) \right). \quad (8)$$

It is clear that the field near the origin represents a magnetic dipole inclined by the angle  $\chi_1$ , which rotates in the azimuthal direction with  $\phi = \Omega t$ .

The electromagnetic fields for a rotating magnetic quadrupole are similarly described by

$$B_r = \frac{Q}{8r^4} \left[ 12P_2^0(\chi_2)P_2^0(\theta) + 4P_2^1(\chi_2)P_2^1(\theta)S_3(\xi)e^{i\lambda_2} + P_2^2(\chi_2)P_2^2(\theta)S_3(2\xi)e^{2i\lambda_2} \right], \quad (9)$$

$$B_\theta = -\frac{Q}{24r^4} \left[ 12P_2^0(\chi_2)P_2^{\prime 0}(\theta) + 4P_2^1(\chi_2)P_2^{\prime 1}(\theta)S_4(\xi)e^{i\lambda_2} + P_2^2(\chi_2)P_2^{\prime 2}(\theta)S_4(2\xi)e^{2i\lambda_2} \right], \quad (10)$$

$$B_\phi = -\frac{iQ}{4r^4} \left[ 2P_2^1(\chi_2) \cos \theta S_4(\xi)e^{i\lambda_2} + P_2^2(\chi_2) \sin \theta S_4(2\xi)e^{2i\lambda_2} \right], \quad (11)$$

$$E_\theta = -\frac{Q\Omega}{4cr^3} \left[ P_2^1(\chi_2) \cos \theta S_3(\xi)e^{i\lambda_2} + P_2^2(\chi_2) \sin \theta S_3(2\xi)e^{2i\lambda_2} \right], \quad (12)$$

$$E_\phi = -\frac{iQ\Omega}{24cr^3} \left[ 2P_2^1(\chi_2)P_2^{\prime 1}(\theta)S_3(\xi)e^{i\lambda_2} + P_2^2(\chi_2)P_2^{\prime 2}(\theta)S_3(2\xi)e^{2i\lambda_2} \right], \quad (13)$$

where

$$S_3(\xi) = 1 - i\xi - \frac{1}{3}\xi^2, \quad (14)$$

$$S_4(\xi) = 1 - i\xi - \frac{1}{2}\xi^2 + \frac{i}{6}\xi^3. \quad (15)$$

The phase in eqs. (9)-(13) is shifted by  $\lambda_2 = \lambda + \delta$ , because the meridian plane in which the symmetric axis of the quadrupole is located may differ by the azimuthal angle  $\delta$  from that of the dipole. The near-field of eqs.(9)-(11) for  $R_s \leq r \ll c/\Omega$  at the phase  $e^{i\lambda_2} = 1$  is

$$\mathbf{B} = \frac{3Q}{2r^4}P_2^0(\theta - \chi_2)\mathbf{e}_r - \frac{Q}{2r^4}P_2^0(\theta - \chi_2)\mathbf{e}_\theta = -\nabla \left( \frac{Q}{2r^3}P_2^0(\theta - \chi_2) \right). \quad (16)$$

Thus, the magnetic fields given by eqs. (9)-(11) are those of a rotating quadrupole, whose inclination angle is  $\chi_2$ .

We compare the combination of dipole and quadrupole fields with the case of a pure dipole. A snapshot of almost-closed magnetic field lines near the light cylinder is shown in Fig. 1. Both inclination angles are the same  $\chi_1 = \chi_2 = \pi/4$ , but the meridian planes are perpendicular, that is,  $\delta = \pi/2$ . Field strength is set as  $Q = 0.2\mu c/\Omega$ . It is clear that the quadrupole field is added to the dipole one. The quadrupole field increases more rapidly with the decrease of the radius  $r$ , and dominates for  $r < r_q \approx 0.2c/\Omega$  for the model parameter, since  $B_1 \sim \mu/r^3$  and  $B_2 \sim Q/r^4$ .

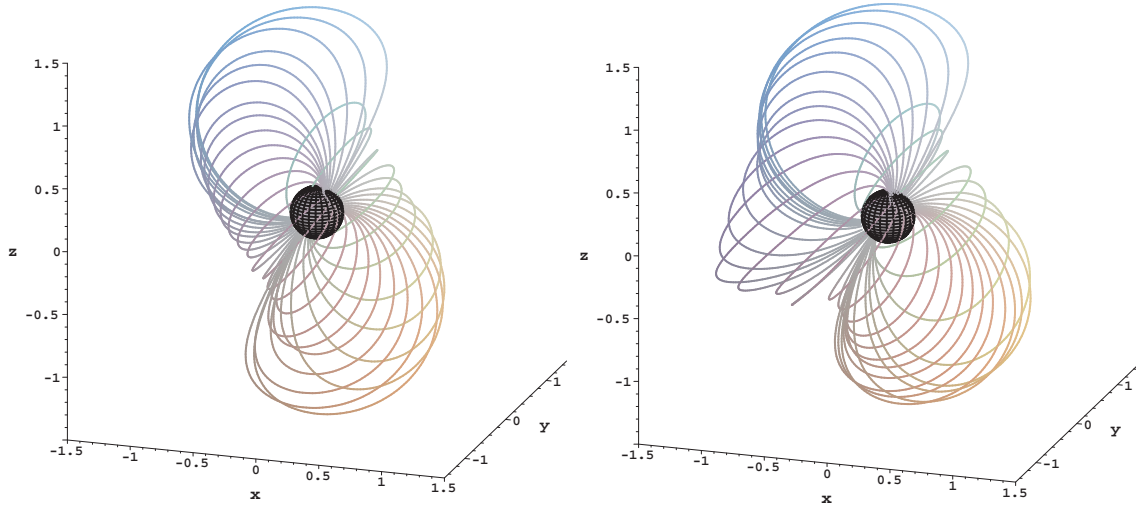


Fig. 1.— Closed magnetic field lines in the cases of pure dipole (left) and dipole plus quadrupole (right). The magnetic axis is inclined by angle  $\chi_1 = \chi_2 = \pi/4$  from the spin axis  $z$ , and the azimuthal angle between moments is  $\delta = \pi/2$ . A sphere of radius  $0.2c/\Omega$  at the origin is also shown. Distance is scaled by  $c/\Omega$ .

## 2.2. Radiation

The radiation energy per unit time is obtained by integrating the time-averaged Poynting flux over the solid angle at the wave zone  $r \gg c/\Omega$ . The luminosity for a combination of electromagnetic fields described by eqs. (1)-(5) and eqs. (9)-(13) is given by

$$L = \int \frac{c}{4\pi} \overline{(\mathbf{E} \times \mathbf{B})} \cdot \mathbf{e}_r r^2 \sin \theta d\theta d\phi = \frac{2\mu^2\Omega^4}{3c^3} \sin^2 \chi_1 + \frac{Q^2\Omega^6}{160c^5} \sin^2 2\chi_2 + \frac{2Q^2\Omega^6}{5c^5} \sin^4 \chi_2. \quad (17)$$

The luminosity is the sum of the contributions from multipole radiation. Our model consists of three components, the magnetic dipole radiation  $M_{1,1}$  specified by spherical harmonics index  $(l, m) = (1, 1)$ , and the quadrupole radiation  $M_{2,1}$  and  $M_{2,2}$ . They correspond to the first, second and third terms in eq. (17). The third term is larger than the second term roughly by a factor  $m^6 = 2^6$ , which comes from the frequency of time variation.

The linear momentum radiated per unit time in the direction  $z$  is similarly calculated as

$$F = \int \frac{1}{4\pi} \overline{(\mathbf{E} \times \mathbf{B})} \cdot \mathbf{e}_z r^2 \sin \theta d\theta d\phi = \frac{\mu Q \Omega^5}{20c^5} \sin \chi_1 \sin 2\chi_2 \sin \delta. \quad (18)$$

The net flux arises from the interference of two multipoles, namely, the magnetic dipole  $M_{1,1}$  and the quadrupole  $M_{2,1}$ . The angle  $\chi_l$  governs the radiation strength of each multiple  $l$ , while the angle  $\delta$  governs the interference. The most efficient configuration is realized when the two magnetic multipole moments are orthogonal,  $\delta = \pi/2$ . On the other hand, when both of the multipole moments lie in the same meridian plane (i.e.,  $\delta = 0$ ), the net linear momentum vanishes. This property can be understood from the fact that radiative electromagnetic fields in vacuum are expressed by the spherical Hankel function  $h_l$  and the asymptotic form for  $\xi = \Omega r/c \gg 1$  is  $h_l \sim \exp[i(\xi - l\pi/2)]/r$  for the multipole  $l$ . There is a phase shift  $\pi/2$  between dipole and quadrupole fields, and this shift is important in the wave interference.

## 2.3. Comparison

We compare our result with the off-center dipole model (Harrison & Tademaru 1975; Lai, Chernoff & Cordes 2001). The rates of energy and linear momentum are written in term of the magnetic dipole moment  $(\mu_R, \mu_\phi, \mu_z)$  in cylindrical coordinate and distance  $s$  from the spin axis as follows:

$$L = \frac{2\Omega^4}{3c^3} (\mu_R^2 + \mu_\phi^2) + \frac{4\Omega^6}{15c^5} s^2 \mu_z^2. \quad (19)$$

The first term is the magnetic dipole radiation  $M_{1,1}$ . Correspondence to our expression is clear by replacing  $\mu_R^2 + \mu_\phi^2 = \mu^2 \sin^2 \chi_1$ . The second term is derived from the sum of electric dipole radiation  $E_{1,1}$  and magnetic quadrupole radiation  $M_{2,1}$ . Their contributions are  $\Omega^6 s^2 \mu_z^2 / (6c^5)$  by  $E_{1,1}$  and  $\Omega^6 s^2 \mu_z^2 / (10c^5)$  by  $M_{2,1}$ , respectively. The parameter in the off-center dipole model corresponds to  $Q \sin 2\chi_2 = 4s\mu_z$  except for a complex phase factor. There is a constraint on the quadrupole

moment  $Q$  as  $Q \sin 2\chi_2 \leq 4\mu R_s \cos \chi_1$ , since  $s \leq R_s$ . In our model, it is possible to consider the case of  $Q \gg \mu R_s$  in magnitude.

The linear momentum in the off-center dipole model is evaluated as (Lai, Chernoff & Cordes 2001)

$$F = \frac{8\Omega^5 s \mu_\phi \mu_z}{15c^5}. \quad (20)$$

Net linear momentum flux arises from two types of interference. One is between magnetic dipole radiation  $M_{1,1}$  and electric dipole radiation  $E_{1,1}$ . The other is between magnetic dipole radiation  $M_{1,1}$  and magnetic quadrupole radiation  $M_{2,1}$ . These contributions are expressed by  $\Omega^5 s \mu_\phi \mu_z / (3c^5)$  and  $\Omega^5 s \mu_\phi \mu_z / (5c^5)$ , respectively. The latter reduces to eq. (18) if  $s \mu_z = Q \sin 2\chi_2 / 4$  and  $\mu_\phi = \mu \sin \chi_1 \sin \delta$ .

Although there is a slight difference in the radiative components between the off-center dipole and dipole-quadrupole models, both formulae for eqs. (17),(18) and eqs. (19),(20) are parameterized as

$$L = \alpha \frac{\mu^2 \Omega^4}{c^3} + \beta \frac{Q^2 \Omega^6}{c^5}, \quad (21)$$

$$F = \frac{\gamma}{10} \frac{\mu Q \Omega^5}{c^5}, \quad (22)$$

where  $\alpha$ ,  $\beta$  and  $\gamma$  are dimensionless numbers that depend on only the geometrical configuration. The typical values are listed in Table 1 for the simple assumption that  $\sin \chi_l, \sin \delta \rightarrow 1/\sqrt{2}$ , that is, the directional average of  $\langle \sin^2 \chi_l \rangle = \langle \sin^2 \delta \rangle = 1/2$ . It is clear that the coefficient  $\beta$  in our model is considerably larger than that in the off-center model. This comes from the radiation of  $m = 2$ .

### 3. EVOLUTION

We next consider the evolution of spin and kinetic velocity. The angular velocity  $\Omega(t)$  is determined by equating the loss rate of rotational energy with the luminosity  $L$  in eq. (21), and the velocity  $V(t)$  is determined from the momentum emission  $F$  in eq. (22). In terms of the mass  $M$  and inertial moment  $I$ , we have

$$I\Omega\dot{\Omega} = -\alpha \frac{\mu^2 \Omega^4}{c^3} - \beta \frac{Q^2 \Omega^6}{c^5}, \quad (23)$$

Table 1: Comparison of models.

Model	Multipole	$\alpha$	$\beta$	$\gamma$	$\gamma/(\alpha\beta)^{1/2}$
Off-center dipole	$M_{1,1}, M_{2,1}, E_{1,1}$	0.33	$0.83 \times 10^{-2}$	0.47	9.0
Dipole-quadrupole	$M_{1,1}, M_{2,1}, M_{2,2}$	0.33	0.10	0.18	0.97

$$M\dot{V} = -\frac{\gamma}{10} \frac{\mu Q \Omega^5}{c^5}. \quad (24)$$

By using the approximation  $I = 2MR_s^2/5$ , where  $R_s$  is the stellar radius, the magnitude of the velocity gained from the initial angular velocity  $\Omega_i$  is given by

$$\Delta V = \frac{\gamma Q R_s^2}{25\mu} \int_{\Omega_0}^{\Omega_i} \frac{\Omega^2}{\alpha c^2 + \beta(Q/\mu)^2 \Omega^2} d\Omega \leq \Delta V_* \equiv \frac{\gamma}{25c(\alpha\beta)^{1/2}} (\Omega_i R_s)^2 X^{-2} [X - \tan^{-1} X], \quad (25)$$

where  $X \equiv (\beta/\alpha)^{1/2} Q \Omega_i / \mu$  and the present angular velocity  $\Omega_0 = 0$  is used in the last inequality. The function  $\Delta V_*$  is determined by the ratio  $Q/(\mu R_s)$  of the two multipole moments for the fixed geometrical configuration and the initial angular velocity  $\Omega_i$ . Two limiting cases of  $\Delta V_*$  are approximated as

$$\frac{\Delta V_*}{c} \approx \begin{cases} \frac{\gamma}{75\alpha} \left(\frac{Q}{\mu R_s}\right) \left(\frac{\Omega_i R_s}{c}\right)^3 & \text{for } 0 < X \ll 1 \\ \frac{\gamma}{25\beta} \left(\frac{Q}{\mu R_s}\right)^{-1} \left(\frac{\Omega_i R_s}{c}\right) & \text{for } X \gg 1. \end{cases} \quad (26)$$

The value  $\Delta V_*$  increases as the ratio  $Q/(\mu R_s)$  increases, while  $Q/(\mu R_s) \ll 1$ , but begins to decrease for  $Q/(\mu R_s) \rightarrow \infty$ . Thus, it has a maximum with respect to the magnetic moment ratio:

$$\frac{\Delta V_*}{c} \approx 9.2 \times 10^{-3} \frac{\gamma}{(\alpha\beta)^{1/2}} \left(\frac{\Omega_i R_s}{c}\right)^2 \quad \text{at} \quad \frac{Q}{\mu R_s} \approx 1.5 \left(\frac{\alpha}{\beta}\right)^{1/2} \left(\frac{\Omega_i R_s}{c}\right)^{-1}. \quad (27)$$

The magnetic moment ratio at the maximum means that the quadrupole field  $B_2 \sim Q/R_s^4$  is stronger than the dipole field  $B_1 \sim \mu/R_s^3$  at the surface. The energy loss rate  $L_l$  of each multipole is approximately the same at the beginning,  $L_2 = \beta Q^2 \Omega_i^6 / c^5 \approx 2.3 \times \alpha \mu^2 \Omega_i^4 / c^3 = 2.3 L_1$ , but the contribution of  $L_2$  and becomes smaller as  $\Omega$  is decreased. The velocity using the canonical values is evaluated as

$$\Delta V_* \approx 120 \left(\frac{P_i}{1\text{ms}}\right)^{-2} \times \frac{\gamma}{(\alpha\beta)^{1/2}} \text{ km s}^{-1} \quad (28)$$

For the off-center dipole model,  $V_* \sim 10^3 (P_i/1\text{ms})^{-2} \text{ km s}^{-1}$  is allowed for an initially rapid rotator, the initial period  $P_i = 1 \text{ ms}$ , using typical values given in Table 1. On the other hand, the typical value is small,  $V_* \sim 10^2 (P_i/1\text{ms})^{-2} \text{ km s}^{-1}$ , for the dipole-quadrupole model. The difference comes from the presence of radiation of  $m = 2$ , which causes efficient energy loss, as discussed in the previous section. Nevertheless, extremely high velocity is possible for a specific configuration even in the present model. Small  $\beta$  corresponds to high velocity. For small  $\chi_2$  in eq. (17), we have  $\beta = \sin^2 2\chi_2/160$ . Because  $\alpha = 2\sin^2 \chi_1/3$ ,  $\gamma = \sin \chi_1 \sin 2\chi_2/2$  for  $\sin \delta = 1$ ; the combination of parameters reduces to  $\gamma/(\alpha\beta)^{1/2} = 7.7$ . The resultant kick velocity increases up to  $\sim 930 (P_i/1\text{ms})^{-2} \text{ km s}^{-1}$ . This optimal case corresponds to the magnetic configuration with an inclined dipole and a nearly axially symmetric quadrupole. The ratio of the moments is  $Q/(\mu R_s) \sim 74(\sin \chi_1 / \sin \chi_2)(P_i/1\text{ms})$ .

Time evolution of spin and velocity is calculated for the optimized relation (27). Once the quadrupole field strength is fixed, the evolution of  $\Omega(t)$  in eq.(23) is scaled by characteristic time

$t_*$  of the dipole radiation loss for the initial angular velocity  $\Omega_i = 2\pi/P_i$ :

$$t_* = \frac{Ic^3}{\alpha\mu^2\Omega_i^2} \approx 0.8 \left( \frac{\alpha}{0.33} \right)^{-1} \left( \frac{P_i}{1\text{ms}} \right)^2 \left( \frac{\mu}{10^{31}\text{Gcm}^3} \right)^{-2} \text{ yr} , \quad (29)$$

where magnetic dipole field at the surface is chosen as  $B_1 \sim 10^{13}$  G. Figure 2 shows the evolution of  $\Omega(t)/\Omega_i$  as a function of  $\tau = t/t_*$ . The ratio of quadrupole to the total energy loss rate,  $L_2/(L_1 + L_2)$  is also plotted. The ratio at  $t = 0$  is approximately 0.7 because of  $L_2 \approx 2.3L_1$ , but monotonically decreases. At  $t = t_*$ , the angular velocity becomes  $\Omega \sim 0.5\Omega_i$  and the contribution of quadrupole radiation also decreases as  $L_2 \sim 0.5L_1$ . The velocity  $V(t)$  normalized by the terminal one (eq.(28)) is also shown in Fig.2. The magnitude attains to almost terminal value,  $V \sim 0.8\Delta V_*$  before  $t = t_*$ .

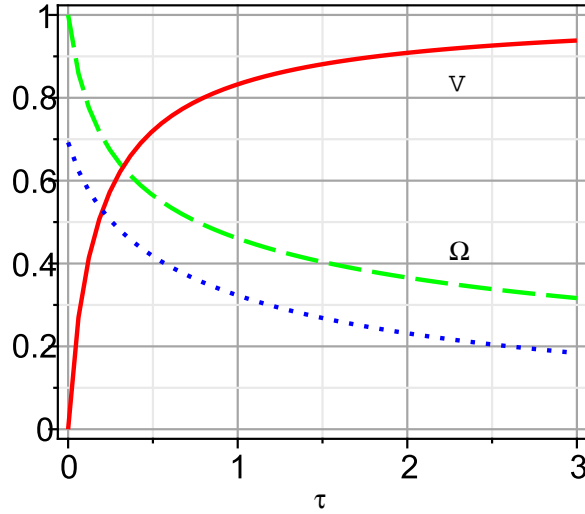


Fig. 2.— Time evolution of velocity, spin and energy loss rates as a function of dimensionless time  $\tau = t/t_*$ . Solid line represents the linear velocity normalized by the terminal one  $\Delta V_*$ , and dashed line the angular velocity normalized by initial one  $\Omega_i$ . Dotted line is the radiation loss ratio  $L_2/(L_1 + L_2)$ .

#### 4. CONCLUSIONS

Magnetic field strength itself is critical in most kick mechanisms. For example,  $B_s > 10^{15}$  G at the surface is required in asymmetric neutrino emission (e.g., Arras & Lai (1999)), as well as in asymmetric magnetized core collapse (e.g., Sawai, Kotake & Yamada (2008)). The resultant velocity increases with the field strength because the asymmetry arises from the magnetic field. Magnetars are therefore expected to have high velocity if one of these mechanisms is operative. Recent observations do not support the high velocity. Rather, the upper limit of the transverse



velocity  $v_{\perp}$  has been reported, although there is uncertainty in the value. For example,  $v_{\perp} \sim 210 \text{ km s}^{-1}$  for AXP XTEJ1810-197 (Helfand et al. 2007),  $v_{\perp} < 1300 \text{ km s}^{-1}$  for SGR 1900+14 (Kaplan et al. 2009; De Luca et al. 2009) and  $v_{\perp} < 930 \text{ km s}^{-1}$  for AXP 1E2259+586 (Kaplan et al. 2009). For fast moving pulsars, PSR2224+45 ( $v_{\perp} > 800 \text{ km s}^{-1}$  Cordes, Romani & Lundgren (1993)) and B1508+55 ( $v_{\perp} \sim 1000 \text{ km s}^{-1}$  Chatterjee et al. (2005)) have been reported. These magnetic fields are quite ordinary,  $B_s = 2.7 \times 10^{12} \text{ G}$  and  $2.0 \times 10^{12} \text{ G}$ , respectively. Thus, there is no clear correlation between the field strength and the velocity in the present sample.

The electromagnetic rocket mechanism considered in Harrison & Tademaru (1975) and in this paper does not depend on field strength if the spin evolution is determined from the radiation loss. In our model, the ratio of dipole and quadrupole moments is important. The condition for high velocity is that the quadrupole field is large enough in magnitude for the radiation loss to be of the same order as the dipole field. The velocity also depends on the geometrical configuration of the multipole moments, that is, each inclination angle from the spin axis and the angle between the axes of symmetry of the moment. Assuming that the directions of moments are random, and that they are equally likely to be oriented in any direction, it is found that the mean velocity with respect to the configuration is not so large,  $\sim 120(P_i/1\text{ms})^{-2} \text{ km s}^{-1}$ , for the optimized dipole-quadrupole ratio. The maximum velocity is realized for a specific configuration in which the inclination angle of the quadrupole moment is small, and the meridian plane in which the quadrupole moment lies is perpendicular to the plane of the dipole. The velocity increases up to  $\sim 930(P_i/1\text{ms})^{-2} \text{ km s}^{-1}$ . This value is slightly smaller than the maximum observed velocity of a pulsar.

The configuration is unknown, and is closely related to the origin of the magnetic field, dynamo or fossil. Nevertheless, Bonanno, Urpin & Belvedere (2006) reported interesting results within the mean-field dynamo theory. They argued that strong large-scale and weak small-scale fields are generated only in a star with a very short initial period, that is, the Rossby number is small, and that the maximum strength decreases and small-scale fields become dominant with the decrease of the initial period. Thus, magnetars may have an ordered dipole with a strong field, while some pulsars may have rather irregular fields with higher multipoles. Through the superposition of higher multipoles, pulsars in general come to have a larger radiation recoil velocity than magnetars.

Finally, if the kick velocity of pulsars and magnetars is governed by the same mechanism, it either should not simply depend on magnetic field, or should depend on only the configuration. The latter possibility was explored here. Present argument is recognized as the order of magnitude level due to the rotating model in vacuum. Further improvement of the magnetosphere will be of importance to explore the idea.

## Acknowledgements

This work was supported in part by the Grant-in-Aid for Scientific Research (No.21540271) from the Japanese Ministry of Education, Culture, Sports, Science and Technology.

## REFERENCES

- Arras, P., & Lai, D. 1999, ApJ, 519, 745
- Bonanno, A., Rezzolla, L. & Urpin, V. 2003, A&A, 410, L33
- Bonanno, A., Urpin, V., & Belvedere, G. 2006, A&A, 451, 1049
- Chabrier, G., & Küker, M. 2006, A&A, 446, 1027
- Chatterjee, S., Vlemmings, W. H. T., Briskin, W. F., Lazio, T. J. W., Cordes, J. M., Goss, W. M., Thorsett, S. E., Fomalont, E. B., Lyne, A. G., & Kramer, M. 2005, ApJ, 630, L61
- Cordes, J. M., Romani, R. W., & Lundgren, S. C. 1993, Nature, 362, 133
- De Luca, A., Caraveo, P. A., Esposito, P., & Hurley, K. 2009, ApJ, 698, 250
- Dobler, W., Stix, M., & Brandenburg, A. 2006, ApJ, 638, 336
- Fryer, C. L., & Kusenko, A. 2006, ApJS, 163, 335
- Harrison, E. R., & Tademaru, E. 1975, ApJ, 201, 447
- Helfand, D. J., Chatterjee, S., Briskin, W. F., Camilo, F., Reynolds, J., van Kerkwijk, M. H., Halpern, J. P., & Ransom, S. M. 2007, ApJ, 662, 1198
- Jackson, J. D. 1975, *Classical Electrodynamics* 2nd ed., (Wiley, New York)
- Kaplan, D. L., Chatterjee, S., Hales, C. A., Gaensler, B. M., & Slane, P. O. 2009, AJ, 137, 354
- Krolik, J. H. 1991, ApJ, 373, L69
- Lai, D., Chernoff, D. F., & Cordes, J. M. 2001, ApJ, 549, 1111
- Miralles, J. A., Pons, J. A. & Urpin, V. A., 2002, ApJ, 574, 356
- Sawai, H., Kotake, K., & Yamada, S. 2008, ApJ, 672, 465
- Scheck, L., Kifonidis, K., Janka, H.-Th., & Müller, E. 2006, A&A, 457, 963
- Thompson, C., & Duncan, R. C. 1993, ApJ, 408, 194